Application of novelty detection methods to health monitoring and typical fault diagnosis of a turbopump

Lei Hu[1], Niaoqing Hu[1]*, Bin Fan[1] and Fengshou Gu[2]

[1] Laboratory of Science and Technology on Integrated Logistics Support, National University of Defense Technology, China

[2] University of Huddersfield, Queensgate, Centre for Diagnostic Engineering, Huddersfield HD1 3DH, UK

E-mail: hnq@nudt.edu.cn

Abstract. Novelty detection is the identification of deviations from a training set. It is suitable for monitoring the health of mechanical systems where it usually is impossible to know every potential fault. In this paper, two novelty detectors are presented. The first detector which integrates One-Class Support Vector Machine (OCSVM) with an incremental clustering algorithm is designed for health monitoring of the turbopump, while the second one which is trained on sensor fault samples is designed to recognize faults from sensors and faults actually from the turbopump. Analysis results showed that these two detectors are both sensitive and efficient for the health monitoring of the turbopump.

1. Introduction

Turbopump is the propulsion machinery of a large-scale liquid rocket engine (LRE). Once faults of the turbopump occur, they will threaten the safety of the engine. Thus, condition monitoring is important for turbopump to insure reliable operation throughout the course of turbopump's service and ground test [1]. Vibration is a main cause of turbopump destructions and it directly images the condition of the turbopump. Thus vibration monitoring is one of significant ways for turbopump condition monitoring.

Large amounts of vibration datasets have been recorded from different ground tests performed over several years. It has been reported that most of these datasets are from normal operating conditions. However, they do have several occasions when some faults were found in the system. In this scenario because of lack of faulty samples and prior knowledge, a health monitoring system cannot be trained on all possible condition patterns. Thus the recognition of novel or unknown conditions turns to be an effective approach to monitoring the turbopump. Novelty detection, which is also named anomaly detection, identifies new or unknown data that a machine learning system is not aware of during training [1-2]. As novelty detection methods are able to work when only normal data are available, such methods are of considerable promise for health monitoring in the case of lacking fault samples and prior knowledge.

Novelty detection methods that have been used in health monitoring include probability/density estimation methods [2-5], immune system based methods [6], neural networks [2, 7-9], support vector methods [5, 10], etc. For the turbopump in liquid rocket engines, a support vector based novelty

* Corresponding author

detection method, which are named as one-class support vector machines (OCSVMs) and have been studied previously by the authors showed superior performance in separating different faults [11]. However, there are two problems need to be solved. Firstly, an OCSVM should be trained on normal samples in numbers large enough if we want a complete description of normality of the turbopump, while training an OCSVM on samples mounted up to thousands upon thousands will bring high computational burden [12]. Secondly, when applying OCSVM to the turbopump vibration detection, it showed that sensor faults were identified as novel events too. Thus sensor faults should be recognized. Otherwise they can be misinterpreted as turbopump faults and lead to false alarms.

In this paper, two OCSVM detectors will be generated. The first one is used for complete description of normality of the turbopump. In order to solve the learning problem of large samples, OCSVM is integrated with an incremental clustering algorithm that is used to extract a small quantity of representative vectors from large amounts of available samples. The second one trained on sensor fault samples is used for separating sensor faults from faults of the turbopump.

2. Health monitoring

2.1. Novelty Detection Method Integrating OCSVM with Incremental Clustering

2.1.1. Boundary description using OCSVM. OCSVM has two basic descriptions, Tax's hypersphere description [13] and Schölkopf's hyperplane description [14]. The former named support vector data description (SVDD) tries to find a hypersphere that encompasses most feature points in the training set with the minimum radius. Points located outside the sphere will be rejected as outliers. While the latter named υ-support vector classifier (υ-SVC) tries to find a hyperplane separates the dataset from the origin with maximal margin. When the data is preprocessed to have unit norm, υ-SVC is equivalent to the SVDD approach.

Here the SVDD method will be briefly introduced. Suppose $\boldsymbol{X} = \{\boldsymbol{x}_i,\ i = 1,\ 2,\ \cdots,\ l\}$ to be the training set, in which $\boldsymbol{x}_i$ is one of feature vectors and l is the size of the training set. A hypersphere can be obtained by solving the quadratic programming optimization problem

$$\min_{\alpha_i,\alpha_j} \quad P(\alpha) = \sum_{i,j=1}^{l} \alpha_i \alpha_j (\boldsymbol{x}_i \cdot \boldsymbol{x}_j) \tag{1}$$

$$\text{s.t. } 0 \leqslant \alpha_i \leqslant (\upsilon l)^{-1},\ i = 1,2 \cdots,\ l, \tag{2a}$$

$$\sum_{i=1}^{l} \alpha_i = 1 \tag{2b}$$

where α_i and α_j are Lagrange multipliers. The trade-off parameter $\upsilon \in (0, 1)$ is the upper bound on the fraction of outliers over all training samples. And υ can be used to control the trade-off between the volume of the sphere and the number of outliers. Solving such a quadratic problem means finding a set $\{\alpha_i\}$ that minimize $P(\alpha)$ with subject to the constraints of equation (2).

The training vectors with $\alpha = 0$, $0 < \alpha < (\upsilon l)^{-1}$, and $\alpha = (\upsilon l)^{-1}$ are respectively called non-support vectors (NSVs), boundary support vectors (BSVs), and non-boundary support vectors (NBSVs). And they are respectively located in, on and outside the sphere as illustrated in figure 1.

The decision function or test function of SVDD is

$$f(\boldsymbol{z}) = \sum\nolimits_k \alpha_k (\boldsymbol{x}_k \cdot \boldsymbol{z}) - b, \tag{3}$$

where $\boldsymbol{z}$ is a test vector, $\boldsymbol{x}_k$ is one of BSVs or NBSVs and α_k is its corresponding Lagrange multiplier, b is the threshold or offset. If $f(\boldsymbol{z}) \geqslant 0$, $\boldsymbol{z}$ will be accepted as a normal sample, otherwise $\boldsymbol{z}$ will be

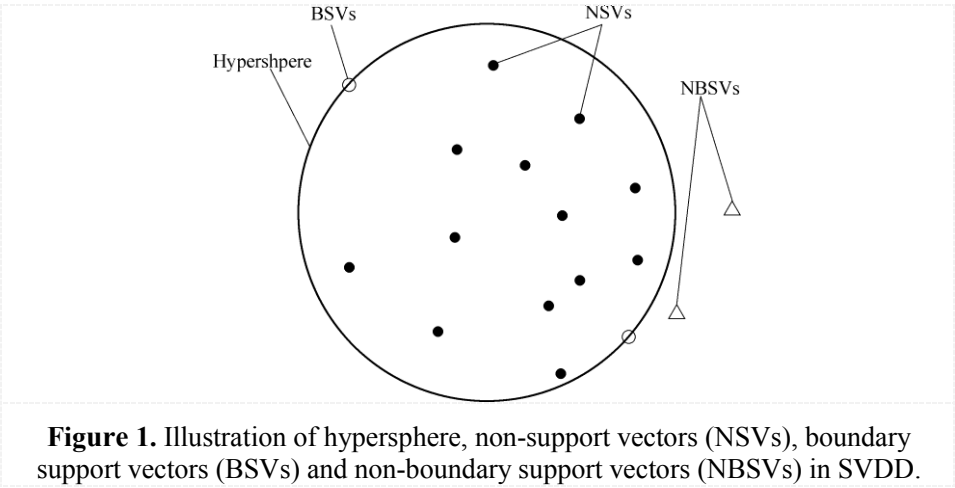

Figure 1. Illustration of hypersphere, non-support vectors (NSVs), boundary support vectors (BSVs) and non-boundary support vectors (NBSVs) in SVDD.

excluded as a novel sample. As BSVs lie on the sphere, the threshold can be yielded by inputting one of BSVs to the decision function

$$b = \delta \sum_k \alpha_k (\boldsymbol{x}_k \cdot \boldsymbol{x}_{\mathrm{BSVs}}), \tag{4}$$

where δ is a scaling parameter used to decrease the threshold to reduce false alarms. δ can be set smaller than and close to 1.

A flexible description can be yielded by replacing the inner product $(\boldsymbol{x}_i \cdot \boldsymbol{x}_j)$ in equations (1), (3), and (4) with a kernel function $K(\boldsymbol{x}_i, \boldsymbol{x}_j)$. And OCSVM mostly uses Gaussian kernel

$$K(\boldsymbol{x}_i, \boldsymbol{x}_j) = \exp(-\frac{\left\| \boldsymbol{x}_i - \boldsymbol{x}_j \right\|^2}{\sigma^2}), \tag{5}$$

where σ is the width parameter of the Gaussian kernel.

2.1.2. Density based Incremental clustering. Density based clustering algorithms are serious candidates for processing large samples as they require only a few passes on the training set and have the merits of high computational efficiency[15]. Here a simple density based incremental clustering algorithm is proposed to extract representative points from large historical test data of the turbopump. When new training samples are available, the cluster described by representative points can be updated incrementally without taking past training set into account.

Define $V_\varepsilon(\boldsymbol{x}_i)$ to be a ε-neighborhood of $\boldsymbol{x}_i$, which is a hypersphere centered at $\boldsymbol{x}_i$ with radius ε defined by user. For any $\boldsymbol{x} \in V_\varepsilon(\boldsymbol{x}_i)$, $\left\| \boldsymbol{x} - \boldsymbol{x}_i \right\| \le \varepsilon$. The "density" of the neighborhood of $\boldsymbol{x}_i$ is the number of points of $\boldsymbol{X}$ lying in $V_\varepsilon(\boldsymbol{x}_i)$, denoted by $N_\varepsilon(\boldsymbol{x}_i, \boldsymbol{X})$. Then two definitions are made as follows.

Definition 1. (dense point and sparse point) A point $\boldsymbol{x}_i$ is a dense point of $\boldsymbol{X}$ if $N_\varepsilon(\boldsymbol{x}_i, \boldsymbol{X}) > q, q \in N$, otherwise it is a sparse point. Here q is the maximum density defined by user.

Definition 2. (the set of representative points) $\boldsymbol{P}$ is a set of $\boldsymbol{X}$'s representative points, if (i) $\boldsymbol{P} \subseteq \boldsymbol{X}$; (ii) $\forall\, \boldsymbol{p} \in \boldsymbol{P}, N_\varepsilon(\boldsymbol{p}, \boldsymbol{X}) \le q$; (iii) $\forall\, \boldsymbol{x} \in \boldsymbol{X}, \exists\, \boldsymbol{p} \in \boldsymbol{P}$, satisfy $\boldsymbol{x} \in V_\varepsilon(\boldsymbol{p})$.

For current novelty detection scheme, there is only one cluster in the algorithm. The set of representative points $\boldsymbol{P}$ can be extracted from training set $\boldsymbol{X}$ using the algorithm as follow.

Let $\boldsymbol{X}^{\mathrm{un}}$ be the set of points in $\boldsymbol{X}$ that have not been considered yet.

Set $\boldsymbol{X}^{\mathrm{un}} = \boldsymbol{X}$, $\boldsymbol{P} = \Phi$

While $\boldsymbol{X}^{\mathrm{un}} \neq \Phi$, do

Arbitrarily select a $\boldsymbol{x} \in \boldsymbol{X}^{\mathrm{un}}$

If $N_\varepsilon(\boldsymbol{x}, \boldsymbol{P}) \leqslant q$, set

$\boldsymbol{P} = \boldsymbol{P} + \{\boldsymbol{x}\}$

$\boldsymbol{X}^{\text{un}} = \boldsymbol{X}^{\text{un}} - \{\boldsymbol{x}\}$

End {if}

End {while}

When a new training set $\boldsymbol{X}^{\text{new}}$ is available, $\boldsymbol{P}$ can be updated by letting $\boldsymbol{X}^{\text{un}} = \boldsymbol{X}^{\text{new}}$, and performing the incremental clustering algorithm. Elder training set $\boldsymbol{X}$ needs not to be considered any more.

In order to process the large data sets in vibration monitoring of the turbopump, density based incremental clustering is used firstly to reduce the size of the training set. In this way, a more representative sample is obtained and presented to OCSVM for more efficient classification.

2.1.3. Parameter tuning. There are four parameters in this novelty detection method:

υ—Trade-off parameter of OCSVM,

σ—Width parameter of Gaussian kernel,

q—Maximum density of $V_\varepsilon(\boldsymbol{x})$,

ε—Radius of $V_\varepsilon(\boldsymbol{x})$.

Determination of parameters υ and σ has been deeply analyzed in Ref. [13]. Generally, a smaller υ should be chosen if few training vector is allowed to be rejected. And σ can be set around $d_{\max}/2$, where $d_{\max}$ is the largest distance between training points. A bigger σ is suggested in fault detection to reduce false alarms on normal data.

For a fixed training set, the choice of q and ε lies on how many representative vectors are supposed to be obtained. Let n be the number of representative vectors extracted. It's not hard to see that the bigger ε, the bigger the region represented by each representative vector, and the smaller the number of vectors needed to represent the complete object region. It's easier to see that the smaller q, the smaller the n for a fixed ε. When $q = 1$, there is only one representative vector in each ε-neighborhood, and representative vectors yielded distribute uniformly in the object region and none of them is redundant. Thus $q = 1$ is suggested first. Then for an acceptable interval $[n_{\min}, n_{\max}]$, the value of ε can be modified according to the number of representative vectors n. Reduce ε to increase n when $n < n_{\min}$ and increase ε to reduce n when $n > n_{\max}$.

2.2. Turbopump Health Monitoring

2.2.1. Feature selection. A mass of vibration signals including a small quantity of fault samples have been recorded from a kind of LRE turbopump in a series of ground tests. Restricted by space and structure, sensors used to record vibrations are mounted on the outside of the turbopump. Vibration signal of the turbopump is a superposition of components and it is hard to recognize faults of the turbopump according to frequency-domain analysis. While faults occur, abrupt shock will arise along with thrust generated by the turbopump. Correspondingly, statistic characteristics of vibration signals will change in the form of energy or waveform. These changes can be described with time-domain features, such as mean, stand deviation, root mean square (RMS), kurtosis factor (KF), clearance factor (CF) and one-step autocorrelation coefficient. Time-domain features have the merit of low cost of computation and they are widely used for monitoring the turbopump of rocket engine in practical engineering. The dependency and fault sensitivity of these time-domain features have been analyzed with a large amount of test data. And RMS, KF and CF are selected finally[16].

Vibration of turbopump is also sensitive to kinds of random factors and its statistic characteristics may vary with tests carried out at different time. In order to enable these detection features to have better consistency and uniform data scaling, the changing rates of RMS, KF and CF instead of themselves are used as final detection features. For a time-domain feature x, its changing rate is

defined as

$$d_x = \frac{x(i+1) - x(i)}{x(i)}. \tag{6}$$

Figure 2 shows the RMS of vibration in test T619 and its changing rates d_{RMS}.

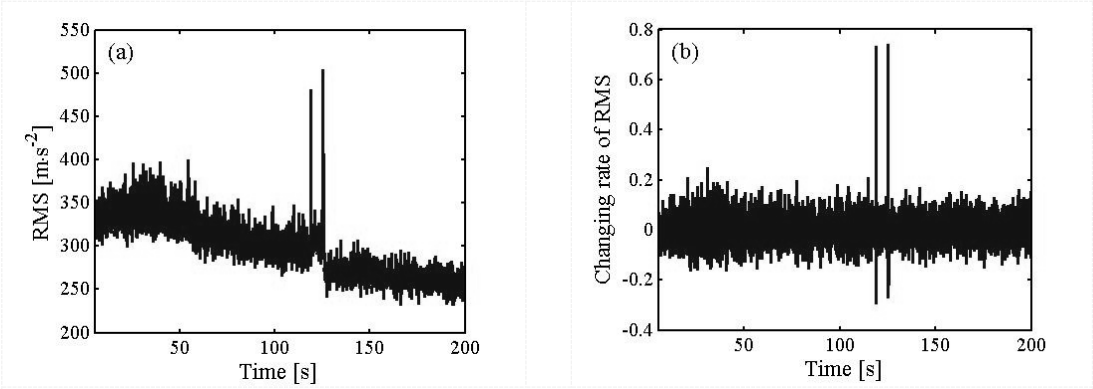

Figure 2. Comparison of (a) RMS and (b) its changing rates d_{RMS}.

2.2.2. Fault detection. Vibration signals of the turbopump were sampled at 50 kHz. Features were calculated every 0.05s. 91 representative points were extracted by performing density based incremental clustering on 36 800 feature vectors. And these 36 800 feature vectors were extracted from 10 historical tests, which are identified by the field engineer to cover various normal operating conditions. The maximum density of $V_\varepsilon(\boldsymbol{x})$ was $q = 1$ and the radius of $V_\varepsilon(\boldsymbol{x})$ was $\varepsilon = 0.12$. A novelty detector was yielded by training OCSVM on these 91 representative points. Parameters of the OCSVM are $\upsilon = 0.01$, $\sigma = 0.8$, $\delta = 0.98$. Then the novelty detector was used to detect abnormality in historical data records.

By taking $f(\boldsymbol{x})$ in equation (3) as novelty index, figure 3 displays the features of test T619. During test T619, turbo vanes shed at 120.83 s and 127.18 s, which caused short shocks in the vibration waveform. But these faults had not been given enough attention. It was fortunate that nasty accident had not been caused and the test continued to the end. Figure 4 shows the novelty indexes of the vibration signal in test T619.

Figure 5 displays the features of test T627 during which serious rub-impact occurred from 11.73 s. Emergency measure was taken to shut down the turbopump. Figure 6 shows the novelty indexes of the vibration signal in test T627.

Figure 7 displays the features of test T618. During test T618, the turbopump itself was normal, but sensor faults occurred. The vibration sensor disabled during time intervals [91.52 s, 93.11 s] and [103.66 s, 104.98 s]. Figure 8 shows the novelty indexes of the vibration signal in test T618.

It can be seen from figure 4, figure 6 and figure 8 that the novelty detector derived from the combination of incremental clustering and OCSVM can detect these kinds of faults effectively. Detection results of all the normal tests that we have (15 tests including those 10 tests used for training the detector) showed no false alarm.

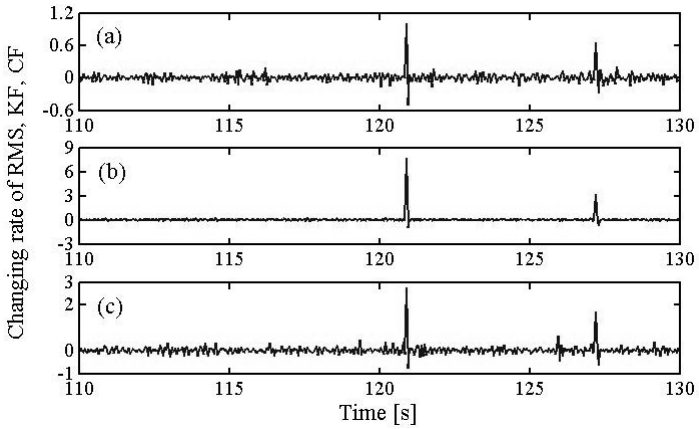

Figure 3. Detection features of test T619: (a) changing rates of RMS, (b) changing rates of KF, (c) changing rates of CF.

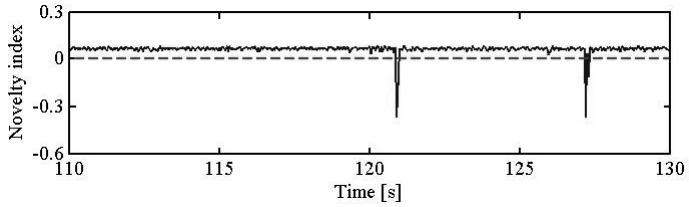

Figure 4. Detection features of test T619.

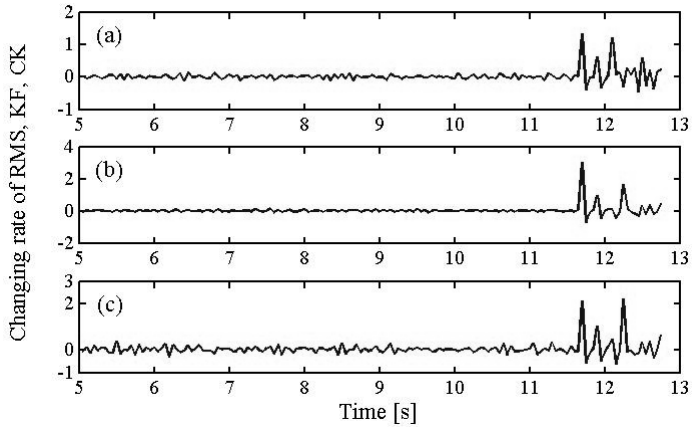

Figure 5. Detection features of test T627: (a) changing rates of RMS, (b) changing rates of KF, (c) changing rates of CF.

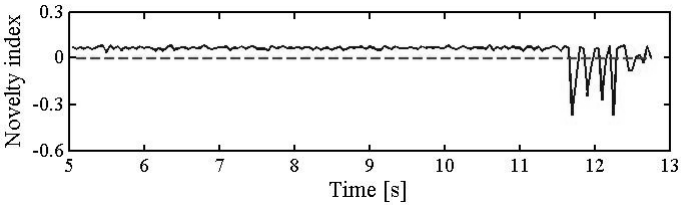

Figure 6. Detection features of test T627.

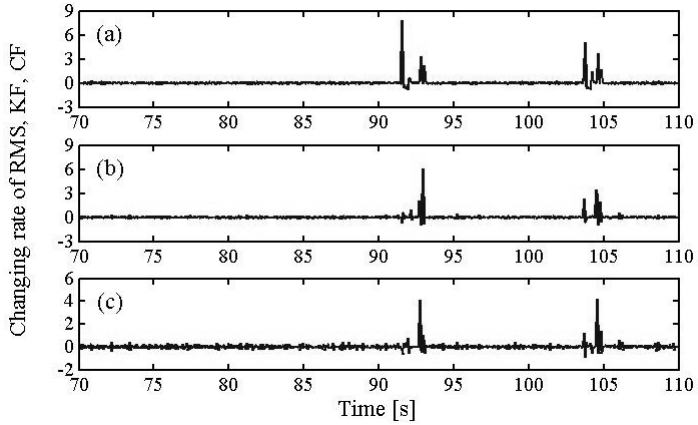

Figure 7. Detection features of test T618: (a) changing rates of RMS, (b) changing rates of KF, (c) changing rates of CF.

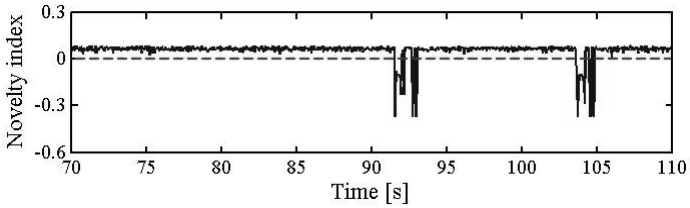

Figure 8. Detection features of test T618.

3. Sensor fault diagnosis

3.1. Feature selection for sensor failure description

Sensors may have abnormalities like bias, drifting, precision degradation, gain variation, et al. Such faults can be detected and corrected in a multichannel measurement system with enough redundant sensors [17]. However, the sensor fault of the turbopump is a different type of malfunction. Figure 9 shows partial typical waveform of the tangential vibration in test T618. There is an excessive negative shock occurring at about 91.9s. Then the accelerometer seems has little output until 93.3s. This abnormal phenomenon also appeared at 104.1s in the same test.

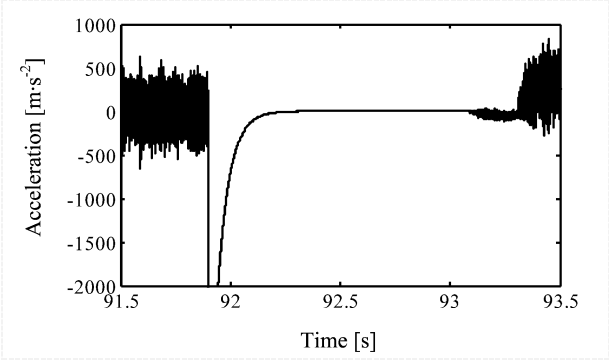

Figure 9. The vibration signal segment during which accelerometer failed.

When the accelerometer has little output, components of vibration from the turbopump cannot be

well sampled and the vibration signal turns to be weak random noise. Figure 10a and 10b show the amplitude spectra of the vibration before and after the sensor malfunction respectively. It is seen that in figure 10b there are a high amplitude lope spreading from 0Hz, indicating that only DC component in the signal when the sensor is in malfunction. On the other head there are high spectral amplitudes in the frequency range from 3000Hz and 7000Hz for the normal sensor case. To describe this difference between two spectra, the standard deviation of spectrum sequence in the frequency range is used as a feature for identifying sensor malfunction. Figure 10c shows the standard deviation of the spectrum (between 3000 Hz and 7000 Hz) of the tangential vibration in test T618. It can be seen that the values for sensor malfunction reduce from about 16 to nearly 0, showing that the standard deviation can be an effective feature.

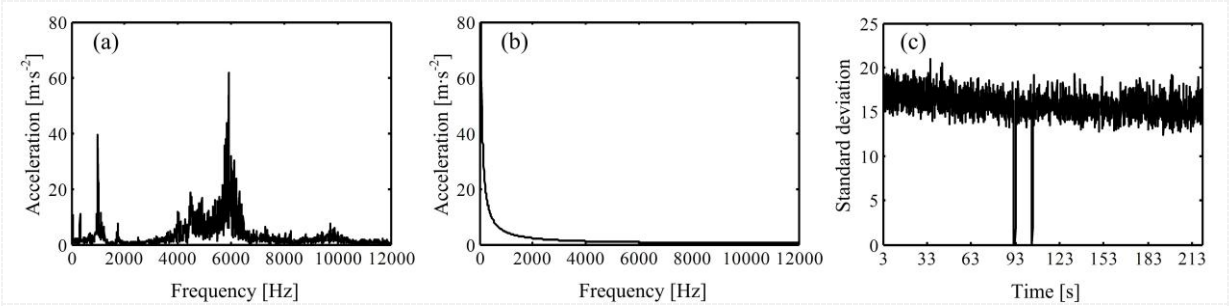

Figure 10. Amplitude spectrum: (a) before sensor malfunction, (b) after sensor malfunction and (c) Standard deviation of the spectrum.

In the meantime, the second feature can be also derived through the correlation analysis between different signals. Although three vibration signals are at three different directions, axial, radial and tangential, as they are sampled synchronously, they should be synchronous correlative to same degree whether the turbopump is normal or not. If one of these sensors is failed, the synchronous correlation between the signal and other signals will decrease significantly. Thus the synchronous correlation can be selected as the feature to recognize sensor malfunction. For two synchronous signals s_i and s_j, their the absolute correlation coefficient $C_{i,j}$ can be calculated by

$$C_{i,j} = \frac{\left|Cov(s_i, s_j)\right|}{\sigma(s_i)\sigma(s_j)} \tag{7}$$

where $Cov(s_i, s_j)$ is the covariance of the two signals s_i and s_j, $\sigma(s_i)$ and $\sigma(s_j)$ are their standard deviations. These two signals are correlative if $C_{i,j} > 0$. They are not correlative if $C_{i,j} = 0$. Figure 11 shows the synchronous correlation coefficients of vibration signals during test T618. It can be seen that the vibration signals are correlative when the sensors are normal. In contrast if one of the sensors fails, the absolute correlation coefficient drops to 0 and the vibration signals are not correlative any more.

3.2. Sensor fault diagnosis results

The accelerometer at axial direction failed many times during ground test T626. During the vibration as shown in figure 12(a), several novelties are found due to moment malfunction of the accelerometer. For developing the SVDD model, the training data is obtained by intercepting these signal segments from the original signal and appending them after each other. Then features are calculated from the training data and its synchronous signal at other directions. The stars in figure 12(b) illustrate the features extracted. The coordinate x_1 is the standard deviation from spectrum and coordinates x_2 and x_3 are respectively the synchronous correlation coefficients of the target vibration signal and its synchronous vibration signals.

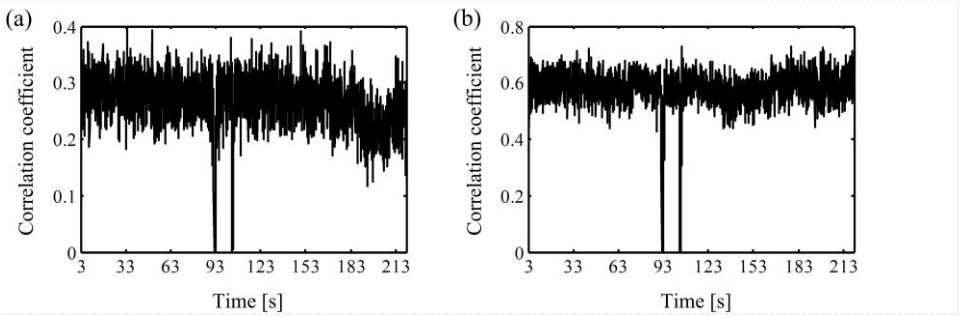

Figure 11. The synchronous correlation coefficients: (a) the correlation coefficient of the tangential vibration and the axial vibration; (b) the correlation coefficient of the tangential vibration and the radial vibration.

According to cross validation results, the parameters of the SVDD are set as $\nu = 0.01$, $\sigma = 2$ and $\delta = 0.98$. Training SVDD with these features yields the description model as shown by the blue grid in figure 12(b). Supposing $f(\mathbf{z})$ is the decision function of the model, which is also the sensor malfunction index, sensor malfunction can be detected if $f(\mathbf{z}) > 0$.

The validity of this description model should be examined in two respects. Firstly, sensor fault should be discriminated from faults of the turbopump. Figure 13 shows the detection results of the tangential vibration in test T618 with the description model using the three features of this vibration in figure 10 and figure 11. It can be seen from figure 13 that the sensor fault index turns to be positive at 91.9s and 104.1s. It means that the novel events detected are identified as sensor malfunction.

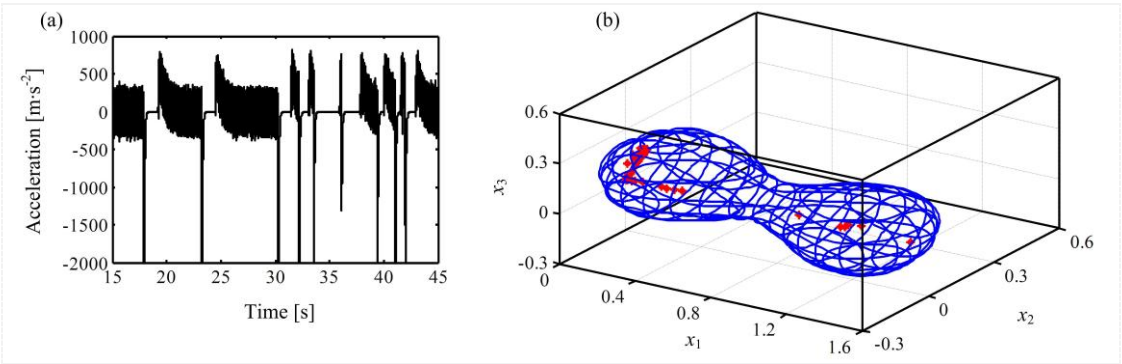

Figure 12. (a) The axial vibration signal of the test T626 during which the accelerometer failed many times, (b) the description of the sensor malfunction: red stars are feature vectors extracted; blue grid is the decision boundary.

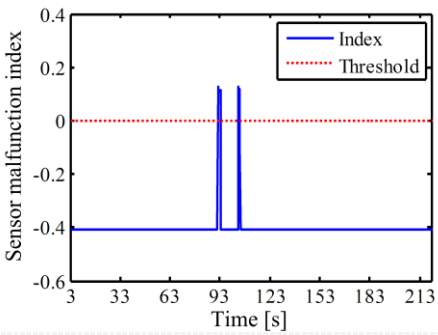

Figure 13. The sensor fault index of the tangential vibration in test T618.

3.3. Discussion

It should be note that sensor disabilities also cause false alarms during online condition monitoring of the turbopump with adaptive Gaussian threshold model. The field engineer does not shut the engine as long as the online monitoring system alarms. The field engineer has to make an aggregate decision according to not only the vibration online monitoring results, but also other factors such as the rotational speed of the turbopump and the hydraulic parameters of the fuel/oxygen fill-in systems. The future research involves hardware embedded online monitoring module for sensor failure detection.

4. Conclusions

In this paper, two novelty detectors are presented for both health monitoring and typical fault diagnosis of the turbopump of a liquid rocket engine.

The first detector is an OCSVM integrated with an incremental clustering algorithm. The incremental clustering algorithm extracts a more representative data set from large historical data sets. By this pre-processing, the data points in the representative set distribute uniformly and cover the entire object region. The detector used for turbopump health monitoring is yielded by training OCSVM on the representative set.

The second detector is an OCSVM trained on sensor fault samples. This detector is used to differentiate sensor faults from the faults of the turbopump. The standard deviation of spectrum and the correlative coefficients of the target signal and its synchronous signals are extracted as the features for sensor fault identification.

By applying these two detectors to full historical datasets, it has produced that all of faults from the turbopump can be detected and can be discriminated from sensor malfunction.

Acknowledgements

The authors are grateful for the financial support from National Natural Science Foundation of China (Grant No. 51105366) and the Specialized Research Fund for the Doctoral Program of Higher Education of China (Grant No. 20114307110017).

References

[1] M. Markou, S. Singh, Novelty detection: a review, Part 1: statistical approaches, *Signal Processing* **83** (2003) 2481- 2497.

[2] K. Worden, G. Manson, D. Allman, Experimental validation of a structural health monitoring methodology, Part I: Novelty detection on a laboratory structure, *Journal of Sound and Vibration* **259** (2003) 323-343.

[3] L. Tarassenko, A. Nairac, N. Townsend, P. Cowley, Novelty detection in jet engines, IEE Colloquium on Condition Monitoring, Imagery, *External Structures and Health* 1999 41-45.

[4] A. Srivastava, Discovering system health anomalies using data mining techniques, in: *Proceedings of the Joint Army Navy NASA Air Force Conference on Propulsion*, Charleston, SC, June 2005.

[5] D. Clifton, P. Bannister, L. Tarassenko, Novelty detection in large-vehicle turbocharger operation, in: *IEA/AIE* 2007 591- 600.

[6] C. Surace, K. Worden, Novelty detection in a changing environment: a negative selection approach, *Mechanical Systems and Signal Processing* **24** (2010) 1114–1128.

[7] S. J. Hickinbotham, J. Austin, Neural networks for novelty detection in airframe strain data, in: *Proceeding of IEEE IJCNN*, 2000.

[8] M. Wong, L. B. Jack, A. K. Nandi, Modified self-organising map for automated novelty detection applied to vibration signal monitoring, *Mechanical Systems and Signal Processing* **20** (2006) 593-610.

[9] P. Hayton, B. Schölkopf, L. Tarassenko, et al., Support vector novelty detection applied to jet engine vibration spectra, in: *Advances in Neural Information Processing Systems* **13**, 2001.

[10] P. Hayton, S. Utete, D. King, et al., Static and dynamic novelty detection methods for jet engine

health monitoring, Philosophical transactions of the royal society, *a-mathematical physical and engineering sciences* **365** (2007) 493-514.
[11] L. Hu, N. Q. Hu, G. J. Qin, Online fault detection algorithm based on double-threshold OCSVM and its application, *Journal of Mechanical Engineering* **45** (2009) 169-173. (in Chinese)
[12] C. Nello, S. John. *An introduction to support vector machines and other kernel-based learning methods*[M]. Cambridge: Cambridge University Press, 2000.
[13] D. Tax, R. Duin, Support vector data description, *Machine Learning* **54** (2004) 45-66.
[14] B. Schölkopf, R. Willianmson, A. Smola, et al. Support vector method for novelty detection[C]. *Advances in neural information processing systems 12: proceedings of the 1999 conference*, MIT Press, 2000: 582–588.
[15] S. Theodoridis, K. Koutroumbs. *Pattern recognition*[M]. 3rd edition. Beijing: China Machine Press, 2006.
[16] G. J. Xie, Research on real-time fault detection technology and system for liquid rocket engine turbopump, Dissertation for doctor's degree at National University of Defense Technology of China, 2006. (in Chinese)
[17] J. Kullaa, Sensor validation using minimum mean square error estimation, *Mechanical Systems and Signal Processing* **24** (2010) 1444-1457.